DESIGN AUDITS

by

J. C. Wachel

President

Engineering Dynamics, Incorporated

San Antonio, Texas

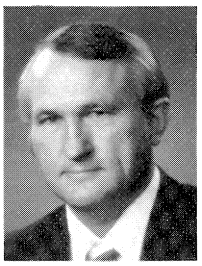

J. C. (Buddy) Wachel is President of Engineering Dynamics, Incorporated, and has over 25 years experience in the solution of vibration and failure problems in rotating and reciprocating equipment and piping. He has performed design audits on numerous new designs and retrofits and is familiar with current technology for analyzing machinery problems.

Mr. Wachel is a member of ASME, ASM, the Vibration Institute, Tau Beta Pi, and Pi Tau Sigma. He holds B.S. and M.S. degrees in Mechanical Engineering from the University of Texas. He has published over 30 technical papers and articles and is a registered professional engineer in the State of Texas.

ABSTRACT

Dynamic design audits of machinery can identify potential problems before the machine is manufactured, thus preventing costly project delays and downtime. The types of audits that should be performed are discussed and typical analysis results are presented along with guidelines as to their interpretation.

INTRODUCTION

The decision to perform a rotordynamic design audit is generally based on the type of machine, the manufacturer's experience with similar sizes, speeds, etc., and the assessment of the benefits relative to the cost of the analysis. If it could be assumed that nothing would go wrong, then the audit would not be needed. However, statistics show that design and manufacturing problems do occur which can result in considerable delay to projects. Cook [1] indicates that over half of the major projects of the past ten years encountered a critical speed design problem and/or high vibration near rated speed. This study indicated that the delay time to correct design equipment error could be as high as 100 weeks. For some performance design error problems, up to four years were needed to correct the problems.

Block [2] states that approximately 22 percent of the unscheduled downtime events for major turbocompressors in process plants are caused by the rotor/shaft systems. Considering all of the unscheduled downtime causes which could be vibration-related, the percentage would be greater than 50 percent. A study by an insurance company found that failures expected each year were about one out of every 186 for steam turbines, and one out of every 26 for gas turbines.

Data such as this and the author's experience in troubleshooting vibration and failure problems indicates that design audits can help prevent many of the problems which are causing unscheduled downtime, project delays, and/or failures by identifying potential problem areas before manufacture.

Another reason for performing an independent audit is the fact that the system may consist of used equipment. In order to avoid any contractual liabilities, the manufacturer may not want to perform the rotordynamic calculations on the new system or the changes that are being made.

Discussion herein is limited to the types of rotordynamic analyses that are commonly performed, the technology available, and typical audit report formats. An outline of the major types of rotordynamic design audits that can be performed is presented in Table 1.

Table 1. Outline of Major Design Audits.

1. Lateral Critical Speed Analyses
   - Critical Speed Map
   - Undamped Natural Frequencies
   - Undamped Mode Shapes
   - Bearing and Seal Stiffnesses and Damping
   - Rotor Response to Unbalance
   - Pedestal and Foundation Effects on Response
   - Stability
2. Torsional Critical Speed Analyses
   - Natural Frequencies
   - Mode Shapes
   - Interference Diagram
   - Coupling Dynamic Torques
   - Dynamic Gear Loads
   - Harmonic Torque Loads for Reciprocating Machinery
   - Torsional Vibrations
   - Shaft Stresses
3. Transient Torsional Analyses
   - Start Up Time
   - Stress Versus Time
   - Cumulative Fatigue
   - Allowable Number of Starts
4. Impeller and Blade Analyses
   - Natural Frequencies
   - Mode Shapes
   - Interference Diagram
   - Experimental Shaker Tests or Modal Analysis
5. Pulsation Analyses
   - Acoustic Resonances
   - Mode Shapes
   - Shaking Forces
   - Surge Effects

LATERAL CRITICAL SPEED ANALYSIS

The most common design audits are the lateral and torsional critical speed audits, since they potentially offer the most benefits. Experience indicates that many systems have been installed with critical speeds in the running speed range, and have run successfully for years before troubles are encountered. This sometimes is difficult to understand, but a design audit that considers the entire range of possible values for the shaft unbalances, bearing and seal parameters will usually indicate the possibility of a problem.

A lateral critical speed audit should include the following calculations:

- Critical speed map
- Undamped natural frequencies and mode shapes
- Bearing stiffness and damping properties
- Seal stiffness and damping properties
- Rotor response to unbalance
- Pedestal and foundation effects on response
- Rotor stability

The first step in performing a lateral critical speed analysis is to model the shaft with sufficient detail and number of masses to accurately simulate the rotor responses through its speed range. An accurate shaft drawing giving the dimensions, weights and center of gravity of all added masses is needed to develop the model. Generally, each significant shaft diameter change is represented by one or more stations. A station is generally located at each added mass or inertia, at each bearing and seal location and at each potential unbalance location. A typical rotor shaft drawing and the computer model are given in Figure 1.

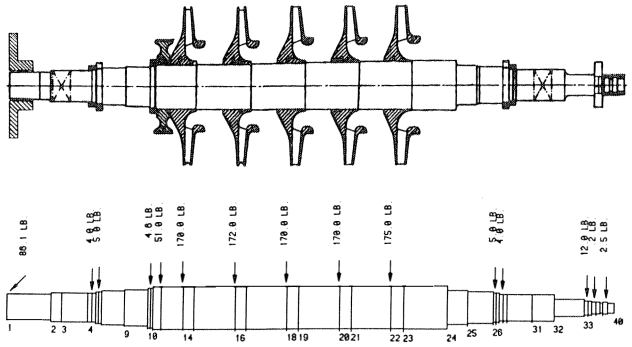

Figure 1. Typical Shaft Drawing and Computer Model.

Rotating elements such as wheels and impellers are modelled as added masses and inertias at the appropriate locations on the shaft. The polar and transverse mass moments of inertia are included in the analysis to simulate the gyroscopic effects on the rotor. The gyroscopic effects are particularly significant on overhung rotors where the impeller or disk produces a restoring moment when whirling in a deflected position.

Couplings are simulated as concentrated added weights and inertias. Normally, the half coupling weight is placed at the center of gravity of the half coupling. When necessary, the entire train, including the driver and driving equipment, can be modelled by utilizing programs which can simulate the shear loading across the coupling without transferring the moments. Once the shaft model is completed, the critical speed map can be calculated.

Critical Speed Map

The critical speed map is a logarithmic plot of the undamped lateral critical speeds *vs* the combined support stiffness, consisting of the bearings and support structures as springs in series. The critical speed map for a seven stage compressor rotor is given in Figure 2. The critical speed map provides the information needed to understand the basic response behavior of rotors; therefore, it is important to understand how the map is developed.

For large values of the support stiffness, the rotor critical speeds are called the rigid bearing critical speeds. If the bearing stiffness if infinity, the vibrations are zero at the bearings, and the first natural frequency for shafts which do not have overhung impellers or disks is analogous to a simply supported beam.

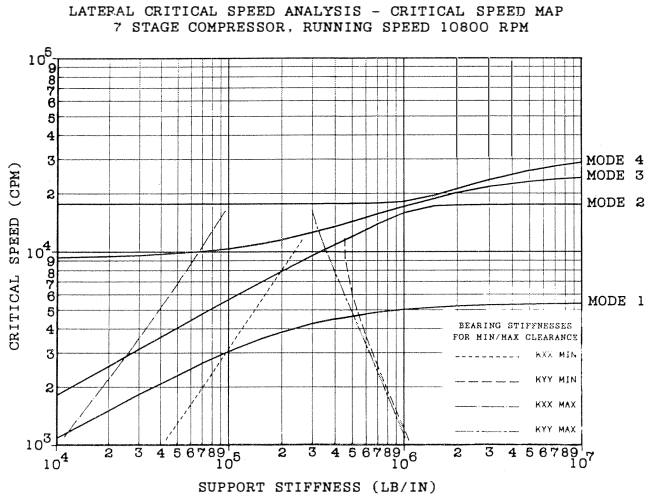

Figure 2. Critical Speed Map for Seven-Stage Compressor.

A normalized critical speed map is given in Figure 3 to illustrate the ratios for the various critical speeds, for low and high support stiffness values, and to illustrate the mode shapes that the rotor will have at different bearing and support stiffness values. For the rigid bearing critical speeds, the mode shape for the first mode would be a half-sine wave (one loop), the second critical speed would be a two loop mode and would occur at four times the first mode critical speed, the third critical speed would be a three loop and would be nine times the first critical, etc. For most rotors, the bearing stiffnesses are less than infinity and the second critical speed will be less than four times the first critical speed and is typically two to three times the first critical speed.

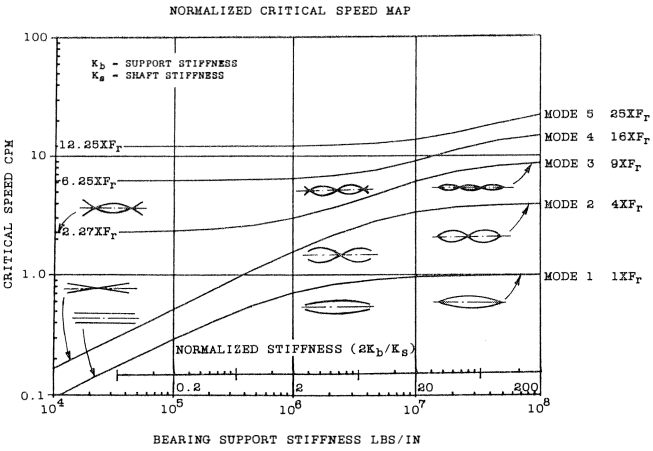

Figure 3. Normalized Critical Speed Map.

For low values of support stiffness (shaft stiffness is large compared to support stiffness), the first critical speed is a function of the total rotor weight and the sum of the two support spring stiffnesses. For an ideal long slender beam, the second mode is similar to the rocking of a shaft on two springs, and is equal to 1.73 times the first critical speed. Since both the first and second modes are functions of the support stiffness, the slope of the frequency lines for the first and second critical speeds *vs* support stiffness is proportional to the square root of the stiffness for low values of support stiffness compared to the shaft stiffness.

For a support stiffness of zero, the third and fourth modes would be analogous to the first and second free-free modes of a beam. For an ideal uniform beam, the ratio of the frequencies

for these modes, compared to the first critical speed for rigid bearings, is 2.27 and 6.25.

Bearings Stiffness and Damping

The dynamic stiffness and damping coefficients of bearings can be adequately simulated using eight linear coefficients (Kxx, Kyy, Kxy, Kyx, Cxx, Cyy, Cxy, Cyx) (Figure 4). This information, along with the lubricant minimum film thickness, flow, power loss, and temperature rise at operating conditions, is needed to evaluate the bearing design. The bearing stiffness and damping coefficients are calculated as functions of the bearing type, length, diameter, viscosity, load, speed, clearance and the Sommerfeld number which is defined as:

$$S = \frac{\mu N D L}{W}\left(\frac{R}{C}\right)^2 \qquad (1)$$

μ = lubricant viscosity, lb-sec/in^2

where

N = rotor speed, Hz
D = bearing diameter, in
L = bearing length, in
R = bearing radius, in
W = bearing load, lbs
C = radial machined clearance, in

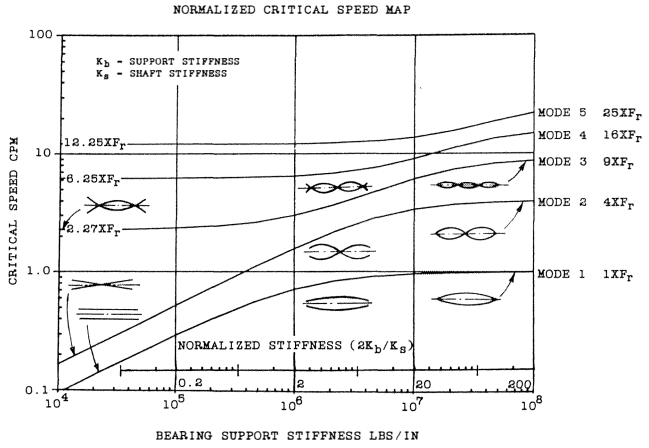

Figure 4. Bearing Stiffness and Damping Coefficients.

Several investigators [3, 4, 5] discuss various types of bearings and their stiffness and damping characteristics. A typical set of bearing calculations is given in Table 2 for a five shoe, load on the pad, tilting pad bearing. The dimensionless coefficients and the actual stiffness and damping values are shown *vs* speed and eccentricity ratio.

The normal procedure in a design audit is to calculate the bearing characteristics for the range of expected clearance, preload and oil temperatures. The maximum clearance, minimum preload and highest oil temperature usually define the minimum stiffness. The other extreme is obtained from the minimum clearance, maximum preload and the coldest oil temperature. This will typically define the range of expected stiffness and damping coefficients for the bearings. An example of the bearing clearances and preloads that can be obtained by considering the range of dimensions of the shaft and bearing is shown in Table 3.

Table 2. Bearing Coefficients for Tilting Pad Bearing.

5 Shoe Tilting Pad Bearing

Load on Pad Arc Length = 52.00 deg		L/D = .42 Pivot Ang. = 54.00 deg			Preload = .444 Offset = .540	
Dimensionless Tilting Pad Bearing Coefficients						
ECC. (dim)	*Sommerfeld (dim)*	*KXX (dim)*	*KYY (dim)*	*CXX (dim)*	*CYY (dim)*	*Torque (dim)*
0.05	3.96E+00	31.352	31.641	34.475	34.677	25.157
0.10	1.96E+00	15.657	16.264	17.144	17.564	25.246
0.15	1.27E+00	10.398	11.355	11.311	11.966	25.397
0.20	9.25E−01	7.740	9.084	8.350	9.257	25.613
0.25	7.09E−01	6.113	7.889	6.530	7.707	25.900
0.30	5.60E−01	4.996	7.254	5.277	6.744	26.265
0.35	4.49E−01	4.162	6.964	4.343	6.120	26.720
0.40	3.62E−01	3.503	6.918	3.607	5.714	27.279
0.45	2.92E−01	2.956	7.072	3.002	5.461	27.963
0.50	2.34E−01	2.486	7.409	2.489	5.320	28.803
0.55	1.85E−01	2.072	7.935	2.045	5.269	29.842
0.60	1.44E−01	1.701	8.678	1.653	5.291	31.144
0.65	1.10E−01	1.366	9.695	1.307	5.375	32.813
0.70	8.04E−02	1.062	11.089	1.000	5.502	35.020
0.75	5.63E−02	0.789	13.046	0.731	5.659	38.078
0.80	3.68E−02	0.548	15.901	0.500	5.875	42.625
0.85	2.17E−02	0.344	20.595	0.310	6.233	50.248
0.90	1.08E−02	0.183	30.649	0.162	7.020	66.733

Dimensional Tilting Pad Bearing Coefficients

L = 1.875 in Load = 438.0 lb		D = 4.500 in		C = .00450 in MU = 2.50E−06 reyns		
ECC. (dim)	*Speed (cpm)*	*KXX (lb/in)*	*KYY (lb/in)*	*CXX (lb/in)*	*CYY (lb/in)*	*HP Loss (hp)*
0.05	19748.2	3.05E+06	3.08E+06	1.62E+03	1.63E+03	6.16E+01
0.10	9744.4	1.52E+06	1.58E+06	1.64E+03	1.68E+03	1.50E+01
0.15	6350.6	1.01E+06	1.11E+06	1.66E+03	1.75E+03	6.43E+00
0.20	4611.7	7.53E+05	8.84E+05	1.68E+03	1.87E+03	3.42E+00
0.25	3535.0	5.95E+05	7.68E+05	1.72E+03	2.03E+03	2.03E+00
0.30	2790.6	4.86E+05	7.06E+05	1.76E+03	2.25E+03	1.28E+00
0.35	2237.0	4.05E+05	6.78E+05	1.80E+03	2.54E+03	8.39E−01
0.40	1804.7	3.41E+05	6.73E+05	1.86E+03	2.94E+03	5.58E−01
0.45	1455.3	2.88E+05	6.88E+05	1.92E+03	3.49E+03	3.72E−01
0.50	1166.3	2.42E+05	7.21E+05	1.98E+03	4.24E+03	2.46E−01
0.55	923.9	2.02E+05	7.72E+05	2.06E+03	5.30E+03	1.60E−01
0.60	719.1	1.66E+05	8.45E+05	2.14E+03	6.84E+03	1.01E−01
0.65	546.0	1.33E+05	9.44E+05	2.22E+03	9.15E+03	6.14E−02
0.70	400.7	1.03E+05	1.08E+06	2.32E+03	1.28E+04	3.53E−02
0.75	280.4	7.68E+04	1.27E+06	2.42E+03	1.88E+04	1.88E−02
0.80	183.2	5.33E+04	1.55E+06	2.54E+03	2.98E+04	8.98E−03
0.85	107.9	3.35E+04	2.00E+06	2.67E+03	5.37E+04	3.67E−03
0.90	53.7	1.78E+04	2.98E+06	2.81E+03	1.22E+05	1.21E−03

Table 3. Clearance Variations with Tolerances.

Dimension	*Minimum*	*Maximum*
Bearing Bore, Inches	*3.0040*	*3.0070*
Journal Diameter, Inches	*2.9990*	*3.0000*
Pad Curvature (Diametrical), Inches	*3.0070*	*3.0090*

CB Mils	*CP Mils*	*Preload M (Dim)*	*Brg. Bore Inches*	*Pad Bore Inches*	*Journal OD Inches*
2.50	4.00	0.3750	3.0040	3.0070	2.9990
2.50	5.00	0.5000	3.0040	3.0090	2.9990
4.00	4.00	0.0000	3.0070	3.0070	2.9990
4.00	5.00	0.2000	3.0070	3.0090	2.9990
2.00	3.50	0.4286	3.0040	3.0070	3.0000
2.00	4.50	0.5556	3.0040	3.0090	3.0000
3.50	3.50	0.0000	3.0070	3.0070	3.0000
3.50	4.50	0.2222	3.0070	3.0098	3.0000

CB is the assembled radial clearance.
CP is the machined radial clearance.
M is the bearing preload factor.

The anticipated range of rotor response should be calculated with the range of bearing values and various combinations of unbalance. This is important since one part of the American Petroleum Institute (API) specifications 617 (2.8.1.9) states:

> If the lateral critical speed as calculated or revealed during mechanical testing falls within the specified operating speed range or fails to meet the separation margin requirements after practical design efforts are exhausted, the unit vendor shall demonstrate an insensitive rotor design. This insensitivity must be proven by operation on the test stand at the critical speed in question with the rotor unbalanced.

The significance of this can be appreciated from the results (Figure 5) of the balanced mechanical test and the sensitivity test for the compressor whose critical speed map was given in Figure 2. It can be seen that the balanced run data showed no troublesome resonances. When the out-of-phase sensitivity tests were made, high amplitude critical speeds were excited.

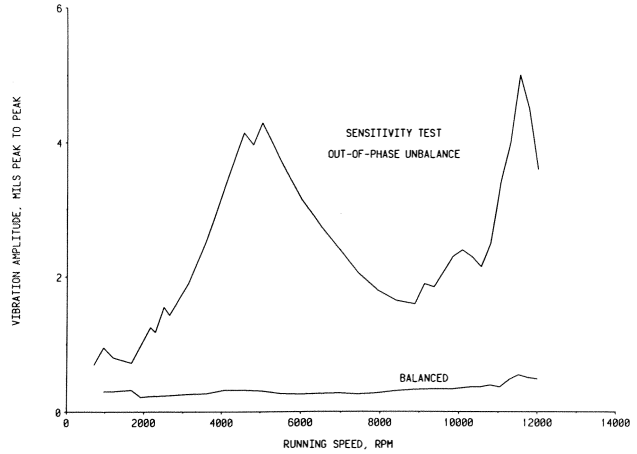

Figure 5. Comparison of Balanced Mechanical Run and Out-of-Phase Unbalance Sensitivity Test.

In the design stage, it is not possible to know the exact installed configuration with regard to bearings (clearance, preload) and balance (location of unbalance). Usually, a mechanical test will be limited to one configuration (clearance, preload, unbalance), which may not show any problem. Changes introduced later, by spare parts during turnarounds, may change sensitive dimensions which may result in a higher response. For this reason, some satisfactorily operating machines change vibration characteristics after an overhaul.

Undamped Natural Frequencies

If the principal bearing stiffnesses are plotted on the critical speed map (Figure 2), the location of the undamped natural frequencies (critical speeds) are identified. By calculating the bearing stiffness and damping coefficients over the expected range of bearing clearances, preload, and viscosity variation, the anticipated range of critical speeds can be estimated. For rotor systems with tilting-pad bearings, which do not have cross-coupling stiffnesses, the measured critical speeds will be near these undamped intersections. For bearings with significant cross-coupling stiffness and damping values, the damped critical speeds are usually higher than the undamped critical speeds.

The vertical and horizontal bearing stiffnesses calculated for the minimum and maximum clearances are plotted on the critical speed map in Figure 2. In this example, the vertical stiffnesses did not change significantly with the change in clearance; however, the horizontal stiffness changed by a factor of four to one. This change illustrates the importance of considering the various combinations of clearances in the calculations. The intersection of these stiffness curves defines the undamped horizontal and vertical critical speeds.

Undamped Mode Shapes

An undamped mode shape is associated with each undamped natural frequency (critical speed) and can be used to describe the rotor vibration characateristics. For a vertical stiffness of 464,000 lb/in, the mode shapes for the first and second undamped natural frequencies are shown in Figures 6 and 7.

The plotted mode shapes were calculated assuming no damping. The actual vibration mode shapes and response frequencies

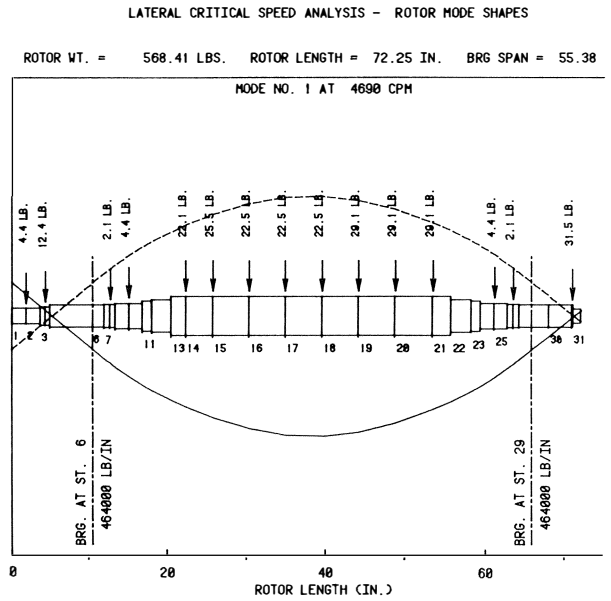

Figure 6. Undamped Mode Shape for First Critical Speed.

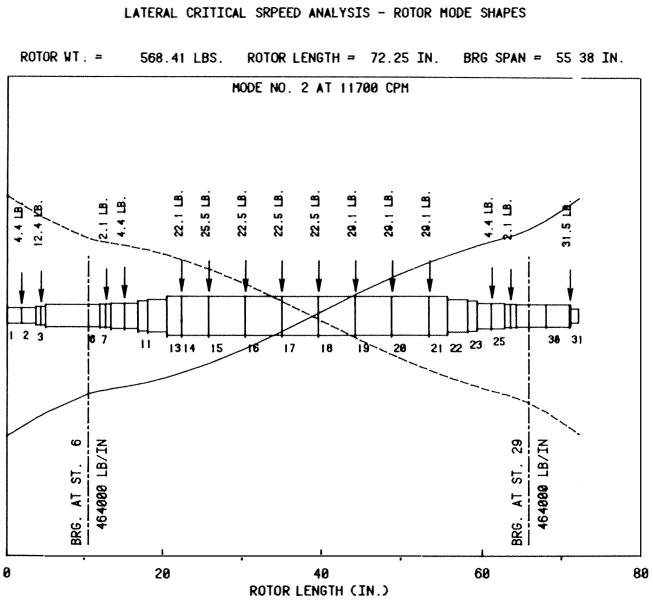

Figure 7. Undamped Mode Shape for Second Critical Speed.

during operation can vary, depending upon the unbalance distribution and damping. The shaft vibrations at any shaft running speed can be calculated for different unbalances using a rotor response program.

Evaluation of Critical Speed Map Calculations

To summarize, in the evaluation of the adequacy of the rotor from the critical speed map and the mode shapes, the following items should be examined:

- *The proximity of the critical speed to the running speed or speed range.* The undamped lateral speeds should not coincide with the running speed. In order to determine if the actual critical speed will cause excessive vibrations, it is necessary to perform a rotor response to unbalance analysis.
- *The location of the critical speed relative to the support stiffness.* If the critical speed is near the rigid bearing critical

speed (flexible shaft region), increasing the bearing stiffness will not increase the critical speed. Also, vibration amplitudes will be low at the bearings, and therefore, low damping will be available. This can contribute to rotordynamic instabilities, which will be discussed later. If the critical speeds are in the area of low support stiffness (stiff shaft region), the critical speeds are stongly dependent upon the bearing stiffness and damping parameters and the critical speeds can shift considerably.

• *The mode shape of the critical speed.* The mode shapes are used to assess the response of the rotor to potential unbalances. For example, a rotor which has a conical whirl mode (second critical speed) would be sensitive to coupling unbalance, but not strongly influenced by midspan unbalance.

Seal Stiffness and Damping Coefficients

In addition to the bearing stiffness and damping effects, the seals and labyrinths can influence the rotor critical speeds and response. Generally, oil ring seals are designed to float with the shaft, since they are held in place by frictional forces dependent upon the pressure balance force and the coefficient of friction. Lubrication and seal oil systems have been discussed by Salisbury, et al [6]. If the seals do not float with the shaft and lock up, they can add additional stiffness and damping. In such cases, they are treated as additional bearings in the rotordynamic calculations. The seal stiffness and damping coefficients are calculated by assuming that the seals are locked at some eccentricity ratio and that the seals are non-cavitating. Typical values of seal stiffness and damping for centrifugal compressors will be less significant than the bearings; however, in some designs they can change the rotor response characteristics.

ROTOR RESPONSE TO UNBALANCE

Computer programs are available today which can calculate the elliptical shaft orbit at any location along the length of a rotor for various types of bearings, pedestal stiffnesses, pedestal masses, seals, labyrinths, unbalance combinations, etc. These programs are used to determine the installed rotor's response to unbalance and predict the critical speeds over the entire range of variables. The actual critical speed locations as determined from response peaks caused by unbalance are strongly influenced by the following factors [7, 8]:

- bearing direct stiffness and damping values.
- bearing cross-coupled stiffness and damping values.
- location of the unbalance.
- location of measurement point.
- bearing support flexibility.

To illustrate the sensitivity of the peak response critical speeds for the compressor whose critical speed map is given in Figure 2, the response due to coupling unbalance and midspan impeller unbalance were calculated. The allowable vibration amplitude (API 617) for this compressor was 1.03 mils peak-to-peak since its maximum continuous speed was 11300 cpm.

The normal unbalance used in an analysis produces a force equal to ten percent of the rotor weight. Usually, rotor response to unbalance calculations are made for midspan unbalance, coupling unbalance, and moment type unbalance. An unbalance equal to a force of five percent of the rotor weight is usually applied at the coupling to excite the rotor. For moment unbalances, an unbalance equal to the five percent of the rotor weight is used at the coupling and another equal unbalance is used out-of-phase on the impeller or wheel furthest from the coupling or on the other coupling if it is a drive-through machine. This type of unbalance was used in the mechanical run sensitivity test shown in Figure 5.

Sensitivity to Bearing Clearance

The computer response analyses for coupling unbalance are given in Figures 8, 9, and 10 for minimum, nominal and maximum clearances, respectively. In order to compare the computer results with the test data, the compressor vibrations were predicted at the two 45-degree probe locations. The vibrations in the horizontal and vertical directions or any other direction can also be predicted. Critical speed responses were predicted at 4800 cpm (well damped) and another critical at 12000 cpm (11 percent above the rated speed of 10800 cpm) for the minimum clearance.

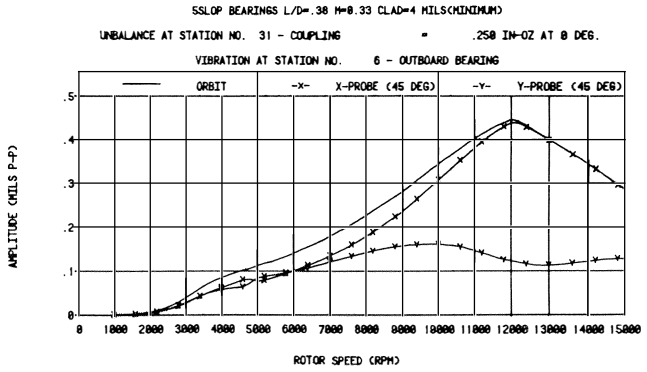

Figure 8. Rotor Response Calculations for Coupling Unbalance and Minimum Clearance.

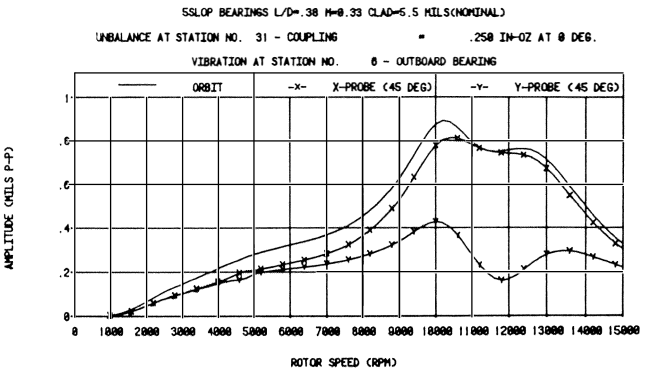

Figure 9. Rotor Response Calculations for Coupling Unbalance and Nominal Clearance.

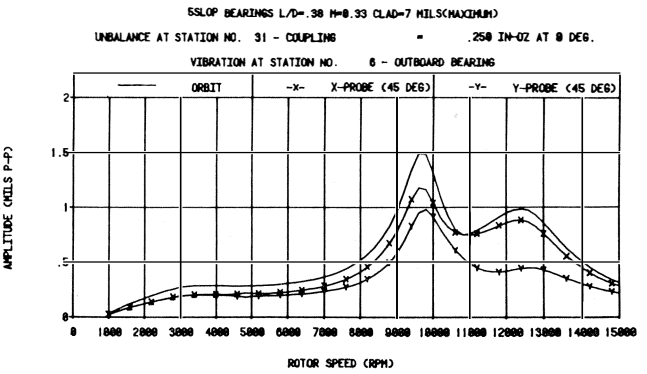

Figure 10. Rotor Response Calculations for Coupling Unbalance and Maximum Clearance.

The predicted amplitudes were less than the API limit for the minimum and nominal clearances. However, when the max-

imum bearing clearance was used, the responses became more pronounced and the predicted amplitudes exceeded the API limits of 1.03 mils. The increased clearance lowered the predicted peak response to 9700 cpm, which is below the rated speed of 10800 cpm.

The predicted unbalance response for midspan unbalance for minimum and maximum clearances is shown in Figures 11 and 12. For minimum clearance, response is noted at the first critical speed near 4800 cpm, with very little response at the second critical speed near 12000 cpm. However, for the maximum clearance, the second critical speed at 9700 cpm becomes the predominant response. This again shows the sensitivity of a rotor to bearing clearance changes.

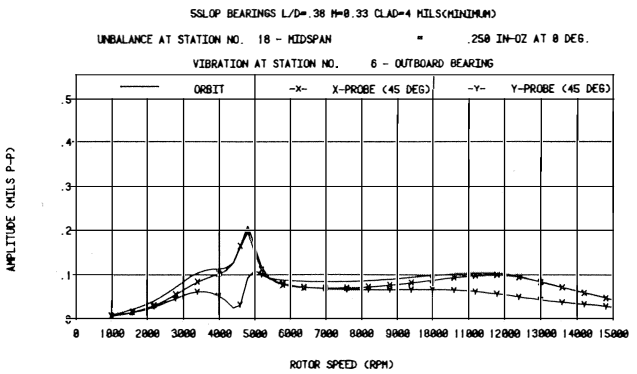

Figure 11. Rotor Response Calculations for Midspan Unbalance and Maximum Clearance.

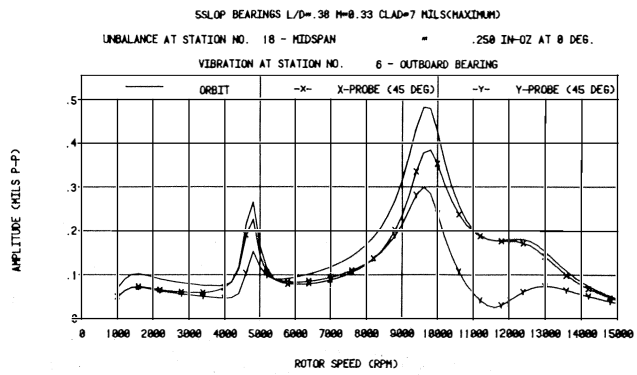

Figure 12. Rotor Response Calculations for Midspan Unbalance on Gas Turbine.

Sensitivity to Unbalance Location

A design audit response analysis was performed on a power turbine with an overhung disk which had a speed range of approximately 2500 cpm to 5000 cpm. The results of the response calculations for unbalance at the coupling are shown in Figure 13. Two peak response critical speeds were excited at 3000 cpm and 5000 cpm. For this unit, very little difference in predicted responses was noted as the bearing parameters were changed. However, when the unbalance was moved to the disk (Figure 14), there were considerable differences in the predicted responses. Note that peak responses at 800 cpm, 2500 cpm, and 5000 cpm are predicted. The two low frequency critical speeds are considerably different from the 3000 cpm mode excited by coupling unbalance.

Sensitivity to Pedestal and Foundation Flexibility

The stiffness, mass and damping of the bearing support structure should be considered in a rotordynamic audit. Basically, the bearing and pedestal stiffnesses combine as springs in series. If the bearing stiffnesses are very low compared to the pedestal stiffnesses, the critical speeds and rotor response will not be greatly affected by the pedestal and support flexibility. Computer programs for dual level rotors are available which can consider the pedestal mass, stiffness and damping values in the rotor response to unbalance calculations.

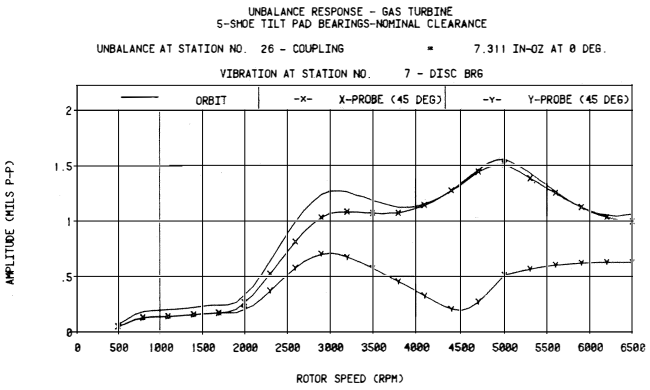

Figure 13. Rotor Response Calculations for Coupling Unbalance on Gas Turbine.

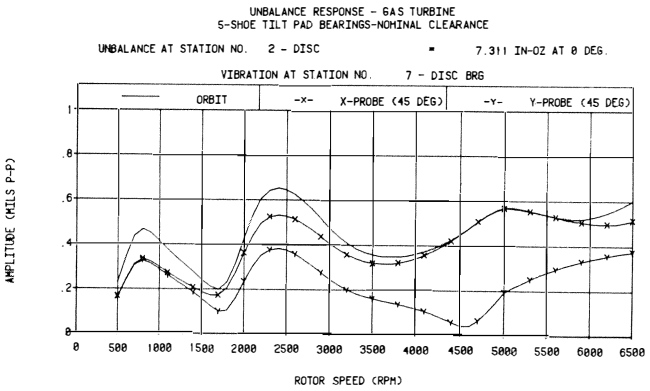

Figure 14. Rotor Response Calculations for Disc Unbalance on Gas Turbine.

In the design stage, the determination of accurate values for the pedestal and supports can be difficult, due to the complex shapes and uncertainties in the bolted joints, grout, and other factors. Finite element programs can be used to determine the needed stiffness and damping values; however, this increases the cost and time of the analysis.

To determine if a complex, finite element analysis of the support structure is needed, parametric runs can be made, varying the support stiffness from large values to values comparable to the bearing stiffnesses. This information will show how sensitive the rotor critical speeds and responses are to pedestal stiffnesses. Generally, pedestal stiffnesses may vary from approximately one million to 20 million lb/in. The horizontal stiffnesses are usually less than the vertical stiffnesses; therefore, the horizontal critical speeds will be lower than the vertical. Pedestal stiffnesses are important in the analysis of large rotors such as induced draft (ID) fans where the pedestal, and foundation stiffnesses will be lower than typical bearing stiffnesses.

Special Lateral Response Analyses

Liquid Pump Lateral Response Analysis

Pump rotordynamics are dependent on a greater number of design variables than are many other types of rotating equipment. Besides the journal bearing and shaft characteristics, the

dynamic characteristics of the seals and the impeller-diffuser interaction can have significant effects on the critical speed location, rotor unbalance sensitivity, and rotor stability [9, 10].

For modelling purposes, seals can be treated as bearings in the sense that direct and cross-coupled stiffness and damping properties can be calculated based on the seal's hydrostatic and hydrodynamic properties. Seal clearances, geometry, pressure drop, fluid properties, inlet swirl, surface roughness and shaft speed are all important in these calculations. Since the pressure drop across seals increases approximately with the square of the pump speed, the seal stiffness also increases with the square of the speed. This increasing stiffness effect is often thought of as a "negative" mass effect, which is usually referred to as the "Lomakin effect" or the "Lomakin mass" [11]. In some cases, the theoretical Lomakin mass or stiffness effect can be of sufficient magnitude to prevent the critical speed of the rotor from ever being coincident with the synchronous speed.

The accurate prediction of the stiffness and damping properties of seals for different geometries and operating conditions is a subject of ongoing research [12, 13]. The basic theories presented by Black [14] have been modified to account for finite length seals, inlet swirl, surface roughness, and other important parameters. However, a universally accepted procedure to accurately predict seal properties is not available for all types of seals in use today. This is particularly true for grooved seals. Unless seal effects are correctly modelled, calculated critical speeds can be significantly different from actual critical speeds.

A series of grooved seal designs used in commercial pumps has been recently tested, and techniques have been developed whereby the seal geometry can be specified and the characteristics calculated for specific assumptions with regard to inlet swirl, groove design, etc. [12, 13].

The rotordynamic analysis of an eight-stage centrifugal pump using serrated (grooved) seals was discussed by Atkins, et al., and will be used to illustrate a design audit of a pump [9]. The first step in a rotordynamic analysis of a pump is to model the basic rotor, using the lumped parameter techniques. A sketch of the rotor with the location of the seals and bearings is given in Figure 15. Note that the pump shaft is analyzed as a rotor with eleven bearings (two cylindrical bearings, eight impellers, and the balance piston).

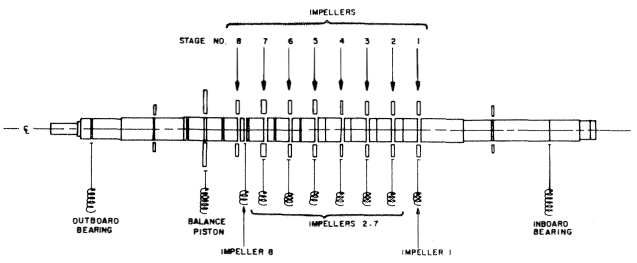

Figure 15. Pump Rotor Model Showing Locations of All Eleven Effective Bearings.

Rotor unbalance response calculations are the key analysis in the design stage for determining whether a pump rotor is acceptable from a dynamics standpoint. In order to bracket the expected range of critical speeds, the unbalance response of a pump should be analyzed for three cases. The first case would have no seal effects and maximum bearing clearances which represent the overall minimum expected support stiffness for the rotor (lowest critical speed). The second case would have minimum seal and bearing clearances, which represents the maximum expected support stiffness and, therefore, the highest critical speed. The third case should be considered with maximum bearing clearances and seal clearances of twice the design clearance to simulate worn seals which represents the pump condition after long periods of service.

The minimum calculated critical speed for the eight-stage pump for the maximum bearing clearancce, no seal case was 1700 cpm (Figure 16). The American Petroleum Institute (API) Standard 610 allowable unbalance was applied at the rotor midspan to excite the first mode. The results of the intermediate (worn seals) case are presented in Figure 17. The worn seals increase the predicted response peak to approximately 1800 cpm. With minimum clearances at the bearings and seals, the frequency increases to 2200 cpm (Figure 18).

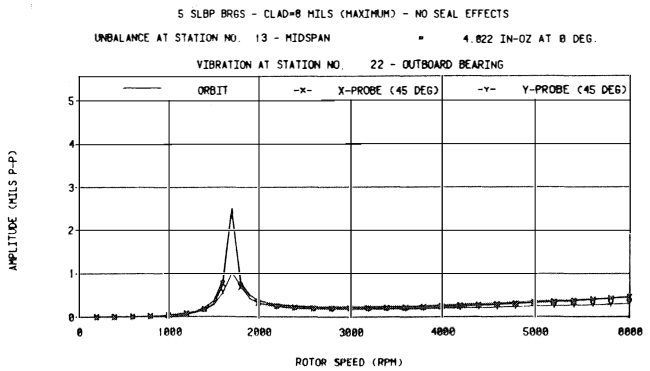

Figure 16. Calculated Unbalance Response at Outboard Bearing for API Unbalance at Midspan. (No seal effects, maximum bearing clearances).

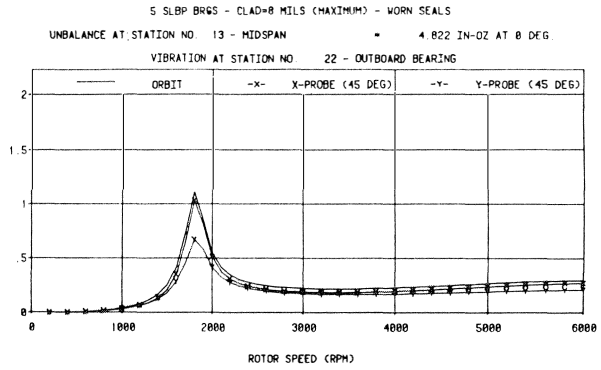

Figure 17. Calculated Unbalance Response at Outboard Bearing for API Unbalance at Midspan. (Maximum (worn) seal clearances, maximum bearing clearance).

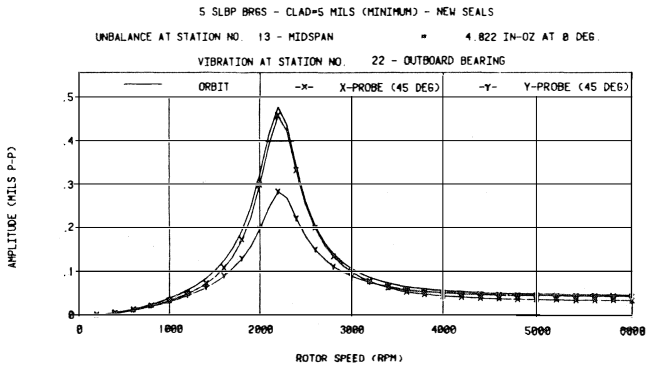

Figure 18. Calculated Unbalance Response at Outboard Bearing for API Unbalance at Midspan. (Minimum (new) seal clearances, minimum bearing clearance).

Gear Shaft Lateral Response Analysis

When performing a lateral critical speed analysis of gear shafts, the effect of the transmitted torque must be considered in the bearing load analysis. API 613 for Special-Purpose Gear Units for Refinery Services (1977) specifies that the critical speeds should not be less than 20 percent above the operating speed. The critical speed, at approximately ten percent, 50 percent, and 100 percent load and maximum continuous speed, should be considered in the calculations.

The relationship of the various forces acting on the gear shaft which has helical gear teeth is shown in Figure 19. Since the bearing forces will depend upon the gear weight and the transmitted horsepower, calculations should be made over the range of ten percent to 100 percent load. Calculations made on a recent audit of a gear are given in Table 4. The gear shafts used four lobed bearings and the bearings stiffnesses and damping changed considerably as the load changed (Table 5). To evaluate the changes in fixed-element bearing properties, rotor response to unbalance calculations must be made.

The effect of load variation for the rotor response can be seen in Figure 20, which gives the response to midspan unbalance for ten percent, 50 percent, and 100 percent load. It can be seen that the critical speed would coincide with the rated speed between 50 percent and 100 percent load.

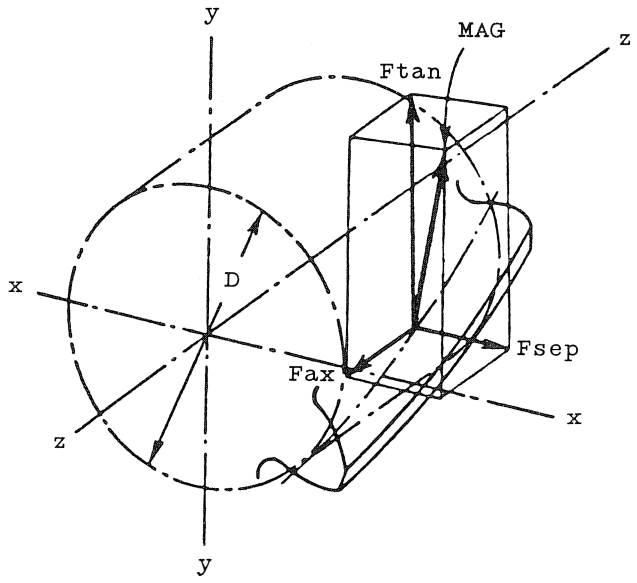

Figure 19. Transmitted Gear Load on Helical Gear Teeth.

Table 4. Bearing Loads as a Function of Transmitted Horsepower.

Horsepower = 31046. bhp
Driver Speed = 5670. cpm
Driven Speed = 10742. cpm
PD Driver = 23.190 in
PD Driven = 12.240 in
Press. Ang. = 20. degrees
Helix Ang. = 14. degrees
Wt Loads: A = −778.0 lb Mesh Dist: A = 14.17 in
B = −1349.0 lb B = 14.17 in
C = −527.0 lb C = 14.17 in
D = −396.0 lb D = 14.17 in
Right Handed Helix on Driver Upmesh—Speed Increaser

				Bull Gear (Driver) Bearing Forces—lb					
% Load	*BRG*	*|Fsep|*	*|Ftan|*	*Fwt*	*Fxnet*	*Fynet*	*MAG*	*DEG*	*Fax*
100.00	A	5568	14875	−778	−2646	−15653	15875	260	7142
100.00	B	5568	14875	−1349	−8490	−16224	18311	242	
75.00	A	4176	11156	−778	−1984	−11934	12098	261	5357
75.00	B	4176	11156	−1349	−6368	−12505	14033	243	
50.00	A	2784	7438	−778	−1323	−8216	8321	261	3571
50.00	B	2784	7438	−1349	−4245	−8787	9758	244	
25.00	A	1392	3719	−778	−661	−4497	4545	262	1786
25.00	B	1392	3719	−1349	−2123	−5068	5494	247	
10.00	A	557	1488	−778	−265	−2266	2281	263	714
10.00	B	557	1488	−1349	−849	−2837	2961	253	

				Pinion (Driven) Bearing Forces—lb					
% Load	*BRG*	*|Fsep|*	*|Ftan|*	*Fwt*	*Fxnet*	*Fynet*	*MAG*	*DEG*	*Fax*
100.00	C	5568	14875	−527	7110	14348	16013	64	−7142
100.00	D	5568	14875	−396	4026	14479	15028	74	
75.00	C	4176	11156	−527	5333	10629	11892	63	−5357
75.00	D	4176	11156	−396	3019	10760	11176	74	
50.00	C	2784	7438	−527	3555	6911	7771	63	−3571
50.00	D	2784	7438	−396	2013	7042	7324	74	
25.00	C	1392	3719	−527	1778	3192	3653	61	−1786
25.00	D	1392	3719	−396	1006	3323	3472	73	
10.00	C	557	1488	−527	711	961	1195	53	−714
10.00	D	557	1488	−396	403	1092	1163	70	

Table 5. Hydrodynamic Bearing Coefficients for Four-Lobed Bearing.

Low Speed Gear
L/D = 0.867 D = 7.086 in. L = 6.14 in
CL = 6.03 mils (nominal) cpm = 5670

Load	Kxx x10^6	Kxy x10^6	Kyx x10^6	Kyy x10^6	Cxx	Cxy	Cyx	Cyy
10%	0.075	0.564	−1.110	1.080	1870	361	315	3780
50%	1.040	0.559	−3.460	5.130	2360	−322	297	12000
100%	2.500	0.972	−7.760	12.400	3880	−1960	−1890	28900

High Speed Pinion
L/D = 1 D = 6.75 in L = 6.75 in
CL = 5.38 mils (nominal) cpm = 10742

Load	Kxx x10^6	Kxy x10^6	Kyx x10^6	Kyy x10^6	Cxx	Cxy	Cyx	Cyy
10%	0.464	−0.175	0.708	0.976	656	14	422	1720
50%	2.090	1.440	3.410	7.310	868	811	2250	8960
100%	5.390	5.090	9.190	19.600	1256	2569	4859	24270

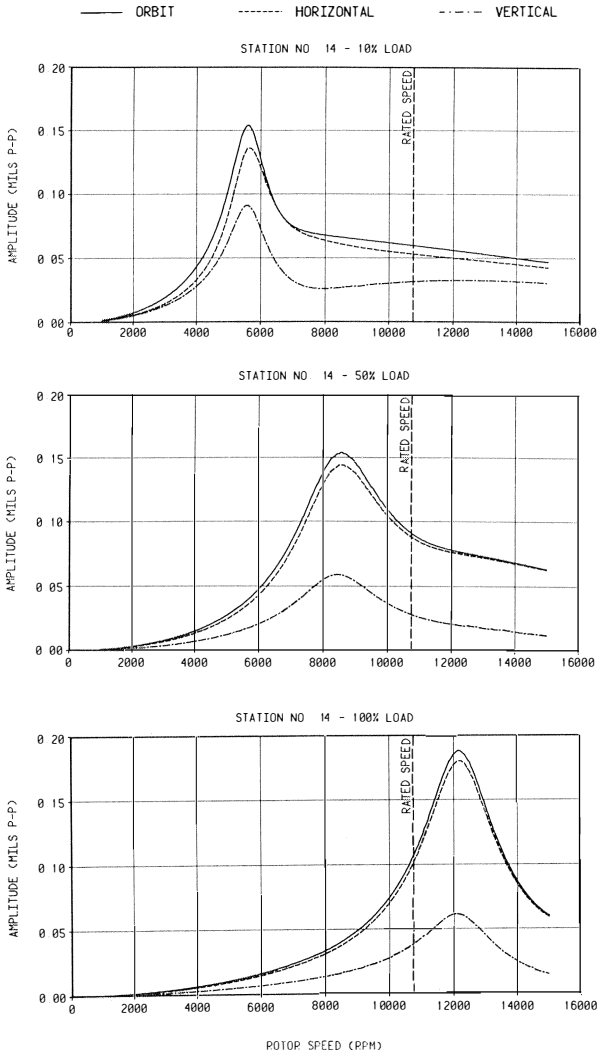

Figure 20. Calculated Pinion Gear Response for Ten Percent, 50 Percent and 100 Percent Load for Midspan Unbalance.

It is often difficult, if not impossible, to meet the required separation margin of API 613 over the entire load range. Generally, the gear shaft and bearing designs are changed to move the critical speeds from the disallowed range for the normal loads. The response analysis is then made to verify that the vibrations will be below acceptable values even if on resonance at the lower loads.

Rotor Stability Analyses

Rotor stability continues to be of major concern, especially for high pressure compressors [15, 16, 17]. Rotor instability occurs when the rotor destabilizing forces are greater than the rotor stabilizing forces. The destabilizing forces can be caused by: the bearings, oil seals, rotor unbalances, friction in shrink fits, or by aerodynamic loading effects such as rotating stall in either impellers or diffusers, impeller blade loading edge incidence, jets and wakes at impeller tips, diffuser stall, pressure pulsations and acoustical resonances, surge, and labyrinth seals.

Instabilities in rotors can cause high vibrations with several different characteristics. They generally can be classified as bearing related, self-excited, and forced non-synchronous instabilities. Oil whirl and half-speed whirl are bearing related instabilities and are caused by the cross coupling from the bearing stiffness and damping in fixed geometry bearings. Half-speed whirl will result in rotor vibrations at approximately one-half of the running speed frequency. Oil whirl describes a special type of subsynchronous vibration which tracks approximately half-speed up to the point where the speed is two times the first critical speed. As the speed increases, the subsynchronous vibration will remain near the first critical speed. These types of instabilities can generally be solved by changing the bearing design to a pressure dam, elliptical, or offset-half bearing, or changing to a tilting pad bearing.

A second type of instability vibrations can occur on any rotor, including those with tilted pad bearings. The vibrations will usually occur near the rotor first critical speed or may track the running speed at some fractional speed. These types of instability vibrations are sometimes called self-excited vibrations, since the motion of the rotor creates the forcing mechanism that causes the instability [18].

A third type of instability is called a forced non-synchronous instability and can be caused by a stage stall in the compressor last stages or by accoustical resonances in the system [19, 20]. This type of instability usually occurs at ten to twenty percent of the running speed as dictated by the acoustical response characteristics of the diffuser and passage geometry.

The predominant method used in performing a stability analysis is to calculate the damped (complex) eigenvalues and logarithmic decrement of rotor, bearing, and seal assembly [21]. A positive logarithmic decrement indicates that a rotor system is stable, whereas a negative logarithmic decrement indicates an unstable system. Experience has shown that due to uncertainties in the calculations, the calculated logarithmic decrement should be greater than 0.3 to ensure stability. The damped eigenvalue and logarithmic decrement are sometimes plotted in a synchronous stability map. Damped eigenvalues generally occur near the shaft critical speeds; however, in some heavily damped rotors, they can be significantly different from the responses due to unbalance.

Rotor stability programs are available which can model the rotor stability for most of the destabilizing mechanisms; however, some of the mechanisms that influence it are not clearly understood [22]. It has been well documented that increased horsepower, speed, discharge pressure, molecular weight and pressure ratio can cause a decrease in the rotor stability. Many units that are stable at low speeds and pressure become unstable at higher values. To predict the stability of a rotor at the design operating conditions, the rotor shaft, bearings, and seals are modelled and the logarithmic decrement is calculated as a function of aerodynamic loading. An equation, based on experience from several instability problems, includes many of the factors which have proved to be important in rotor stability such as horsepower, speed, diameter of impeller, density ratio across the compressor, impeller and diffuser restrictive dimensions, and molecular weight of fluid [15]. This equation can be used to

predict the approximate aerodynamic loading that the unit should be able to withstand. The aerodynamic loading is a cross coupling term, usually applied near the center of the rotor. Conceptually, it can be thought of as a component which detracts from the stabilizing forces in the system.

In the normal audit procedures, the stability is calculated as a function of the aerodynamic loading with a computer model of the rotor, bearings, and seals. In the evaluation of the stability, it is desirable to have a logarithmic decrement at zero aerodynamic loading greater than 0.3 and still greater than 0.1 at the calculated aerodynamic loading. The logarithmic decrement should be calculated for the range of bearing and seal properties expected as shown in Figure 21, in which a plot is presented for the lowest forward mode and indicates the estimated aerodynamic loading.

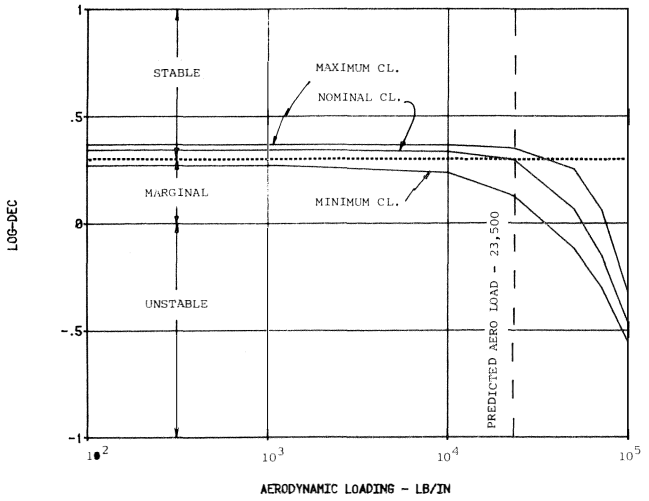

Figure 21. Calculated Logarithmic Decrement vs *Aerodynamics Cross Coupling For Stability Analysis of Centrifugal Compressor.*

Kirk [17] has developed a stability criteria which uses the final pressure times the differential pressure across the machine *vs* the ratio of the running speed to the first critical speed. Stroh [23] suggested a work/energy relationship to determine the aerodynamic loading.

TORSIONAL CRITICAL SPEED ANALYSIS

All rotating and reciprocating systems have torsional vibrations. Operation on a torsional natural frequency can cause shaft failures without an obvious increase in the lateral vibrations. Therefore, it is important to ensure that all torsional natural frequencies are sufficiently removed from excitation frequencies.

A torsional audit should include:

- calculation of the torsional natural frequencies and associated mode shapes.
- development of an interference diagram which shows the torsional natural frequencies and the excitation components as a function of speed.
- calculation of the coupling torques to ensure that the coupling can handle the dynamic loads.
- calculation of shaft stresses, even if allowable margins are satisfied.
- calculation of transient torsional stresses and allowable number of starts for synchronous motor drives.

Torsional natural frequencies are a function of the torsional masses and the torsional stiffnesses between the masses. The natural frequencies and mode shapes are generally calculated by the Holzer method or by eigenvalue-eigenvector procedures. Either of the methods can give accurate results. It is desired that the torsional natural frequencies have a ten percent margin from all potential excitation mechanisms.

An example of the mass-elastic diagram of a torsional system is given in Figure 22. The natural frequencies and mode shapes associated with the first four natural frequencies are given in Figure 23. The mode shapes can be used to determine the most influential springs and masses in the system. This information is important if encroachment is calculated and system changes must be made to detune the systems. Parametric analyses should be made of the coupling stiffness if changes are necessary, since most torsional problems can be solved by coupling changes.

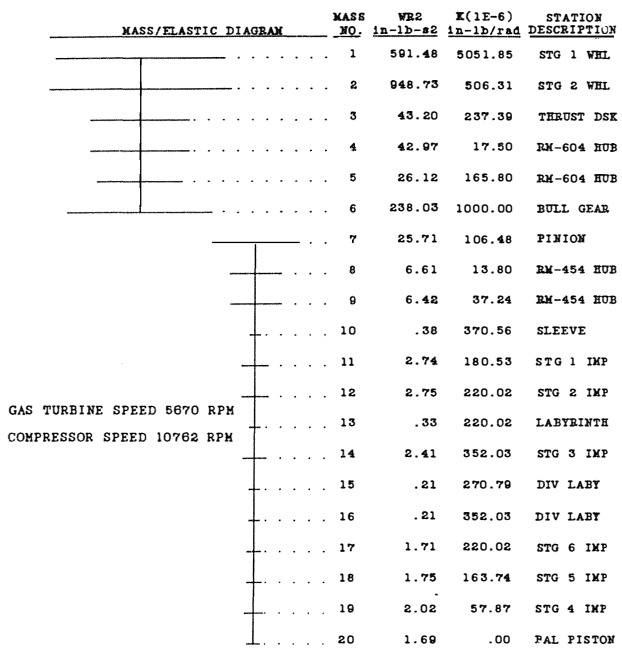

MASS NO.	WR2 in-lb-s2	K(1E-6) in-lb/rad	STATION DESCRIPTION
1	591.48	5051.85	STG 1 WHL
2	948.73	506.31	STG 2 WHL
3	43.20	237.39	THRUST DSK
4	42.97	17.50	RM-604 HUB
5	26.12	165.80	RM-604 HUB
6	238.03	1000.00	BULL GEAR
7	25.71	106.48	PINION
8	6.61	13.80	RM-454 HUB
9	6.42	37.24	RM-454 HUB
10	.38	370.56	SLEEVE
11	2.74	180.53	STG 1 IMP
12	2.75	220.02	STG 2 IMP
13	.33	220.02	LABYRINTH
14	2.41	352.03	STG 3 IMP
15	.21	270.79	DIV LABY
16	.21	352.03	DIV LABY
17	1.71	220.02	STG 6 IMP
18	1.75	163.74	STG 5 IMP
19	2.02	57.87	STG 4 IMP
20	1.69	.00	PAL PISTON

Figure 22. Torsional Mass-Elastic Data for Gas Turbine-Compressor Train.

An interference diagram for the turbine-driven compressor with a gear box is given in Figure 24. The rated speeds are 5670 cpm for the gas turbine and 10762 cpm for the compressor. In this system, excitation at 1× and 2× the gas turbine and compressor speeds are possible. The 1× excitation of gas turbine speed excites the first critical speed at 1907 cpm; however, it will not reach the second natural frequency at 6869 cpm, since the maximum speed would be less than 6000 cpm. The compressor speed (1×) excitation would excite the first torsional natural frequency at 1005 cpm and the second natural frequency at 3619 cpm on the gas turbine.

Once the system has been modelled and the natural frequencies have been determined, the forcing functions should be applied. The forcing functions represent dynamic torques applied at locations in the system which are likely to generate torque variations. Identification of all possible sources of vibration is an important step in diagnosing an existing vibration problem or avoiding problems at the design stage.

The most likely sources of dynamic torques include:

- reciprocating engines, compressors and pumps.
- gears.
- fans, turbines, compressors, pumps.
- motors (synchronous and induction).

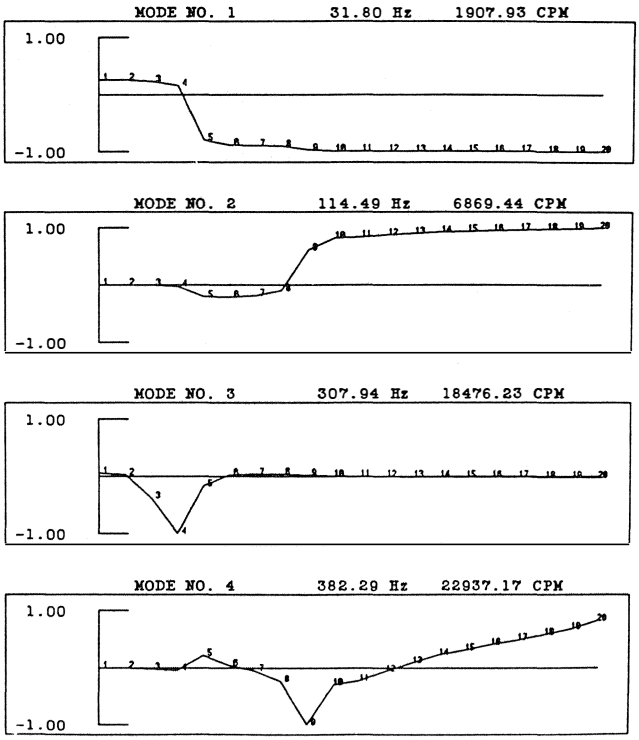

Figure 23. Torsional Natural Frequencies and Mode Shapes.

- couplings.
- fluid interaction (pulsations).
- load variations.

To evaluate the stresses at resonance, the torsional excitation must be applied to the system. For systems with gear boxes, a torque modulation of one percent, zero-peak is a representative torque value which has proven to be appropriate for most cases. As a rule of thumb, excitations at the higher orders for gears are inversely proportional to the order numbers: the second order excitation is 0.5 percent, the third is 0.33 percent, etc.

The torque excitation should be applied at the appropriate location and the torsional stresses calculated on the resonant frequency and at the running speed. An example of the stress calculations of the second natural frequency resonance is given in Table 6. It shows that a one percent torque excitation on the bull gear would cause a maximum torsional stress of 4179 psi peak-to-peak in shaft nine, which is the compressor shaft between the coupling and the first stage impeller. The dynamic torque modulation across couplings are calculated for the applied input modulation. For this mode, the maximum torsional vibrations occur across the compressor coupling and the dynamic torque modulation was 2626 ft-lb.

Table 6. Torsional Stress Calculations at the Second Torsional Natural Frequency for One Percent Excitation at the Bull Gear.

	Dynamic Torques (1 percent Zero-Peak) Applied at the Bull Gear		*Maximum Resultant Torsional Stresses at the 2nd Torsional Resonance 6869.44 cpm*	
Shaft	*Stress PSI P-P*	*scf*	*Stress PSI P-P*	
1	3.92	2.00	7.83	
2	34.47	1.50	51.71	
3	117.23	3.00	351.68	
4	Dynamic Torque Variation		468.82	ft-lb
5	21.76	3.00	65.27	
6*		Gear Mesh		
7	1334.81	3.00	4004.43	
8*	Dynamic Torque Variation		2626.80	ft-lb
9	1393.16	3.00	4179.49	
10	859.02	1.50	1288.52	
11	723.70	1.50	1085.55	
12	582.18	1.50	873.27	
13	564.75	1.50	847.12	
14	434.23	1.50	651.35	
15	422.73	1.50	634.09	
16	411.05	1.50	616.57	
17	314.94	1.50	472.41	
18	215.28	1.50	322.93	
19	98.88	1.50	148.32	

Note: * values are dynamic torque variation across coupling or gear, ft-lb

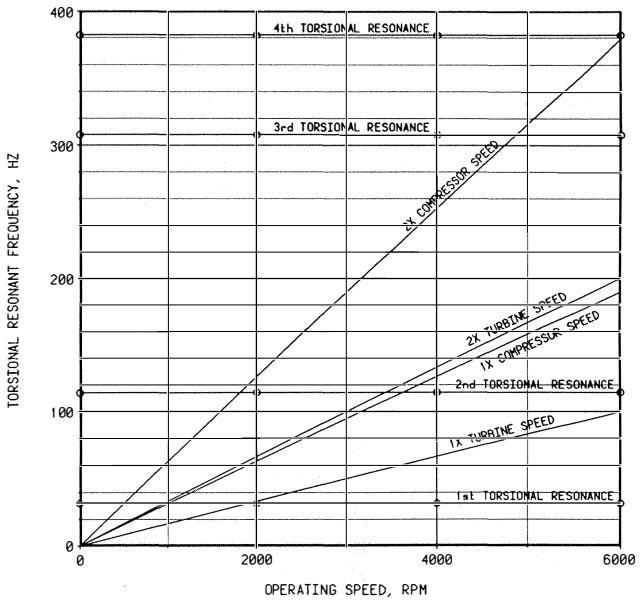

Figure 24. Interference Diagram for Gas Turbine-Compressor Train.

Variable Speed Drives

Units which use a variable speed drive in conjunction with an electric motor will have excitation torques at the running speed frequencies, and at several multiples, depending upon the design of the variable speed drive [24]. An interference diagram for one such system is presented in Figure 25. It is difficult to remove all coincidence of resonances with the excitation sources over a wide speed range; therefore, stress calculations must be made to evaluate the adequacy of the system response.

Reciprocating Machinery

For reciprocating units such as compressors, pumps, or engines, the harmonic excitation torques must be calculated and applied at the appropriate shaft location to calculate the stresses [25].

Allowable Torsional Stresses

The calculated torsional stresses must be compared to applicable criteria. The allowable values given by Military Standards (MIL STD) 164 are appropriate for most rotating equipment. The allowable zero-peak endurance limit is equal to the ultimate

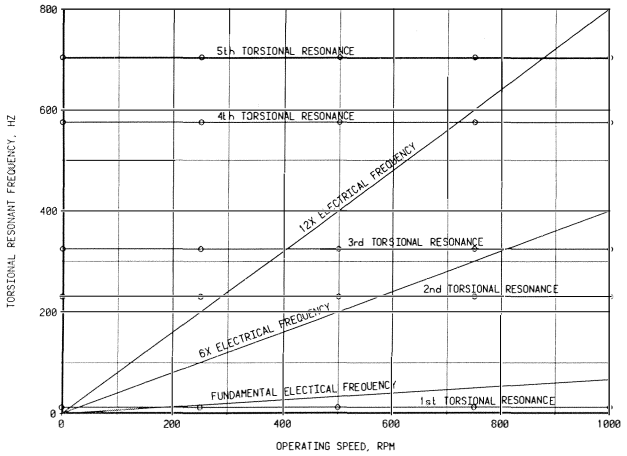

Figure 25. Interference Diagram for Induction Motor with Variable Speed Drive.

tensile strength, divided by 25. When comparing calculated stresses to this value, the appropriate stress concentration factor and a safety factor must be used. Generally a safety factor of two is used for fatigue analysis. When these factors are used, it can be shown that fairly low levels of torsional stress can cause failures, especially when it is realized that the standard (U.S.A. Standard ANSI B17.1) keyway has a stress concentration factor of three. A typical torsional stress allowable thus becomes the ultimate tensile strength divided by 150.

TRANSIENT TORSIONAL ANALYSIS

After the steady state analysis is made, a transient analysis should be made to evaluate the startup stresses and allowable number of startups for synchronous motor systems [22, 26]. The transient analysis refers to the startup conditions which are continually changing, because of the increasing torque and speed of the system. When a synchronous motor starts, an excitation is imposed upon the torsional system due to field slippage. As the motor increases in speed, the torsional excitation frequency decreases from twice power line frequency (typically 120 Hz) linearly with speed toward zero. During this startup, the torsional system will be excited at several of its resonant frequencies, if they are between 0 and 120 Hz, as shown in Figure 26. The response amplitudes and shaft stresses depend upon the resonant frequencies, the average and pulsating torque when the system passes through these resonant frequencies, the damping in the system, and the load torques. The startup analyses can be made for loaded or unloaded operation. The transient response is also affected by the starting acceleration rate of the motor. For slow motor startups, the system will stay at a resonant frequency for a longer period of time, allowing stresses to be amplified. If acceleration is rapid, passing through the resonance quickly will minimize the amplitude increase at resonant frequencies.

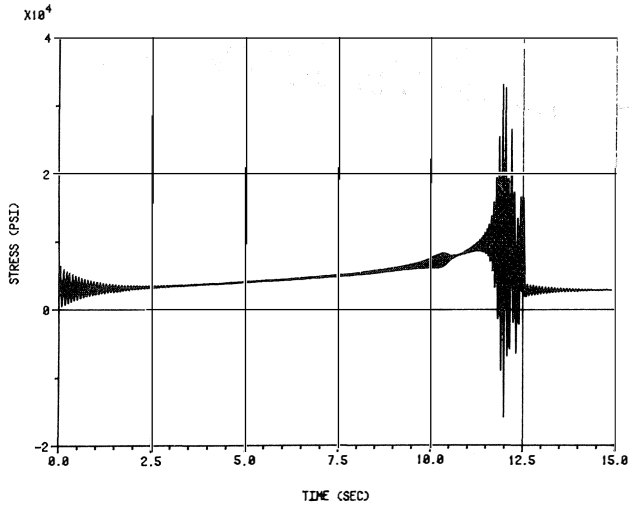

Figure 26. Torsional Stresses Introduced Into Motor Shaft During Synchronous Motor Startup.

Synchronous motors develop a strong oscillating starting torque because of slippage between the rotor and stator fields. Although this is only a transient excitation, the pulsating torque can be strong enough to exceed the torsional endurance limit of the shaft. For this reason, the transient stresses must be calculated and compared to the endurance limit stress. It is not necessary that the transient stresses be less than the endurance limit stress; however, the stresses must be sufficiently low to allow an acceptable number of starts. If the transient stresses exceed the endurance limit, the cumulative fatigue concept is applied to the stresses in excess of the endurance limit stress to determine how many starts can be allowed for the system.

Cumulative fatigue theory is used to estimate the number of cycles a certain stress level can be endured before shaft failure would occur. This is based upon a plot of stress *vs* number of cycles (S-N curve), which defines the stress conditions at which a failure should occur. The S-N curve is based upon actual tests of specimens of a particular type of metal and defines the stress levels at which failures have occurred in these test specimens. These S-N curves are available for most types of shafting materials. Using the appropriate curve, the allowed number of cycles for a particular stress can be determined. The number of total startups which can be made with the system before a shaft failure is predicted, can be calculated. Since the stress levels vary both in amplitude and frequency, a more complex calculation must be made to determine the fraction of the total fatigue which has occurred. The stress levels for each cycle are analyzed to determine the percentage of cumulative fatigue, and then the allowable number of startups can be determined.

The calculation of the allowable number of starts is strongly dependent upon the stress *vs* cycles to failure curve and whether torsional stresses higher than the torsional yield are allowed. In the design stage, it is preferable to design the system such that the introduced torsional stresses do not exceed the yield stresses. This can usually be accomplished through appropriate coupling changes.

IMPELLER AND BLADE RESPONSES

A design audit should also include an assessment of the potential excitation of blade or impeller natural frequencies. Several authors have documented such problems [27, 28, 29, 30]. The impeller and blade response analysis should include:

- the blade and impeller natural frequencies.
- the mode shapes.
- interference diagram indicating potential excitation mechanisms and the natural frequencies.

The interference diagram which gives the blade and impeller natural frequencies and the various potential excitation mechanisms is the key to the prevention of failures. The resonances should be sufficiently removed from the major excitations in the operating speed range.

In the design stage, it is possible to calculate the natural frequencies and mode shapes using finite element method (FEM) computer programs which are available. However, the accuracy of predictions depends to a great extent upon the experience of the analyst and the complexity of the system.

Since the blades and impellers will usually be available in advance of the rotor assembly, the most accurate natural frequency and mode shape data can be obtained from shaker tests or by modal analysis methods. The modal analysis techniques use a two channel analyzer, and an impact hammer and accelerometer to determine the natural frequencies and mode shapes. For example, the natural frequencies and mode shapes of a centrifugal impeller were measured using modal analysis techniques (Figure 27). When these frequencies were compared to values determined from a shaker study, good correlation was obtained. The mode shape for the two diameter mode is given in Figure 28.

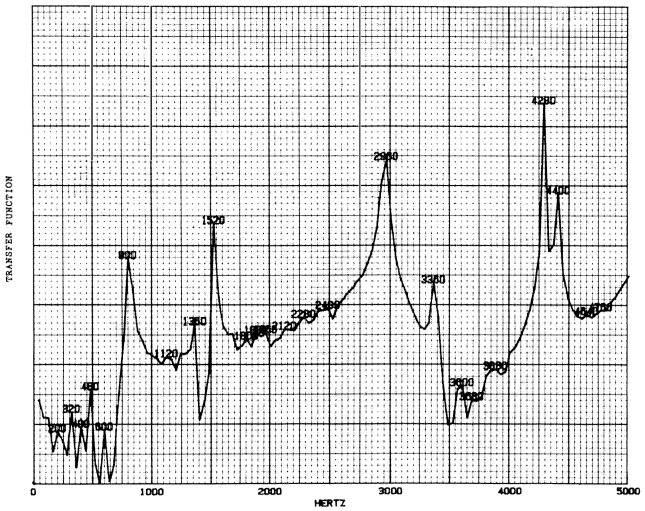

Figure 27. Natural Frequencies of Centrifugal Impeller.

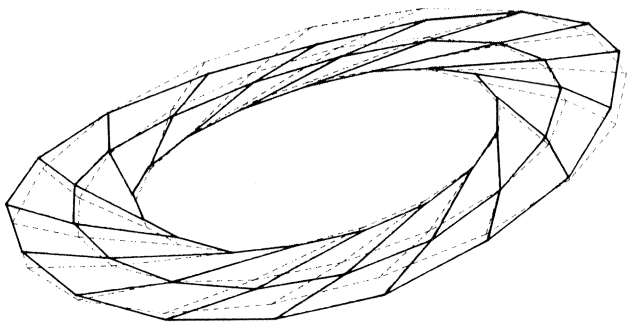

Figure 28. Two Diameter Mode Shape for Centrifugal Impeller at 1360 Hz Determined by Modal Analysis Tests.

An interference diagram for this impeller is given in Figure 29. Note that potential excitation mechanisms include the vane passage frequency (15×) and two times the vane passage frequency (30×).

It is sometimes impossible to completely avoid all interferences over a wide speed range, since there are so many natural frequencies. For most systems, in order for a failure to occur, several things usually occur together. First, there must be a mechanical natural frequency. Second, there must be a definite excitation frequency, such as vane passing or diffuser vane frequency. Third, there must be some acoustical resonant frequency which amplifies the energy generated; and fourth, there must be the appropriate phase relationship that causes the pulsation to cause a shaking force on the impeller or blade. The best way to avoid such problems is to avoid coincidence of the resonances with the excitation mechanisms.

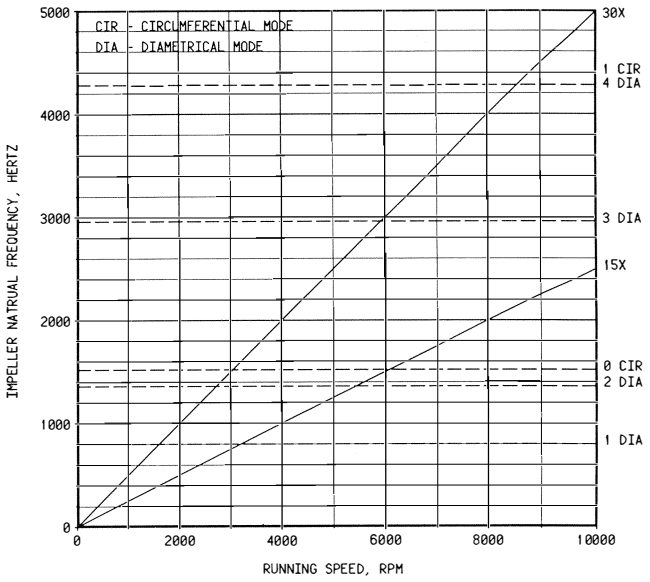

Figure 29. Interference Diagram for Centrifugal Impeller.

PULSATIONS

Pulsations can cause problems in rotating equipment as well as reciprocating machinery. Several case histories were discussed in earlier studies [31, 32]. Pulsation resonances occur in piping systems and are a function of the fluid properties and the piping, compressor, or pump geometry.

Pulsations can cause premature surge in centrifugal compressors and pumps if the generated pulses, such as from stage stall [16]. match one of the pulsation resonances of the system. The potential pulsating excitation mechanisms for piping systems are the running speed component and its multiples, vane and blade passing frequency, and those caused by flow excited (Strouhal frequency) phenomenon [19].

In the design stage, the acoustical natural frequencies of piping systems can be calculated using either digital [25] or analog modelling procedures [31]. A model of a piping system analyzed on a digital computer is given in Figure 30. The predicted pulsations in the reciprocating pump system at selected locations are given in Figure 31. These pulsations levels define the energy in the pump and the piping shaking forces and can be used to define the necessary piping supports and span lengths to achieve acceptable vibration levels. The program can be used to redesign the piping to reduce the pulsations to acceptable levels.

CONCLUSIONS

Typical design audit analyses have been presented, along with some guidelines for determining the need and interpreting the results. It is difficult to determine when an audit is needed; however, it must be thought of as additional insurance that the machinery will run without major problems. Many of the analysis procedures and computer programs that have been developed are being used by both the manufacturer and by consultants who offer these design audit services. As with many computer programs, the interpretation of the computer results is dependent upon the skill and experience of the analyst. The manufacturer produces many machines which have no problems and, thus, has the confidence that the machinery will run successfully. The independent consultant usually is asked to look only at machinery with some kind of problem. Therefore, consultants probably look at the analysis from a slightly different viewpoint. The goal of the manufacturer, the user and the

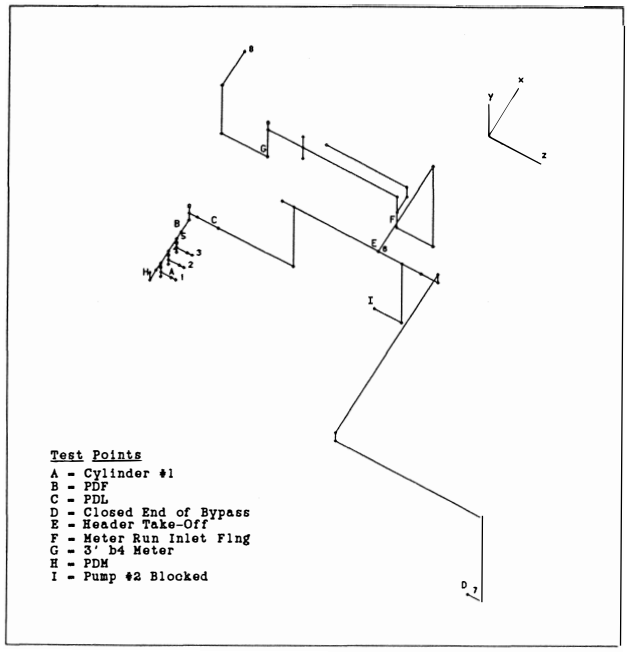

Figure 30. Digital Computer Model of Pump System for Pulsation Analysis.

independent consultant who makes an audit is all the same: everyone wants a trouble-free machine.

The independent audit generally takes place after the manufacturer has finalized his drawings. In many cases where problems were found during the audit, it turned out that after the manufacturer had made his analysis in the initial stages, later some dimensions were changed during the manufacturing, thus causing significant change in the calculated responses. If the independent audit is made, any differences between the manufacturer's and the consultant's calculations can be resolved before installation.

Guidelines as to when an independent audit should be obtained, thus, are dependent upon many factors. Generally audits should be performed on:

- new prototype machines which are extrapolations in horsepower, pressure, number of impellers, bearing span, or new concepts.
- machines which, if unreliable, cause costly downtime.
- machines that are not spared (no backups).
- expensive machines and installations in which the cost of the audit is insignificant compared to total cost.

Typical costs for analyses are difficult to specify, since the scope of the work depends upon the adequacy of the supplied information, the complexity of the machinery, and the number of parametric variation analyses required. If accurate drawings and system information can be supplied to independent consultants who perform these studies, then accurate cost estimates can be given.

Sources of Design Audits

There are several independent consulting companies which can perform all of the discussed design audits. There are also numerous consultants which provide some, but not all, of the analyses, and it would be impossible to list all of them. The sources of the dynamic audits can be obtained from major design, architectural/engineering, oil, chemical, and construction companies which have such firms on their acceptable bidder's list.

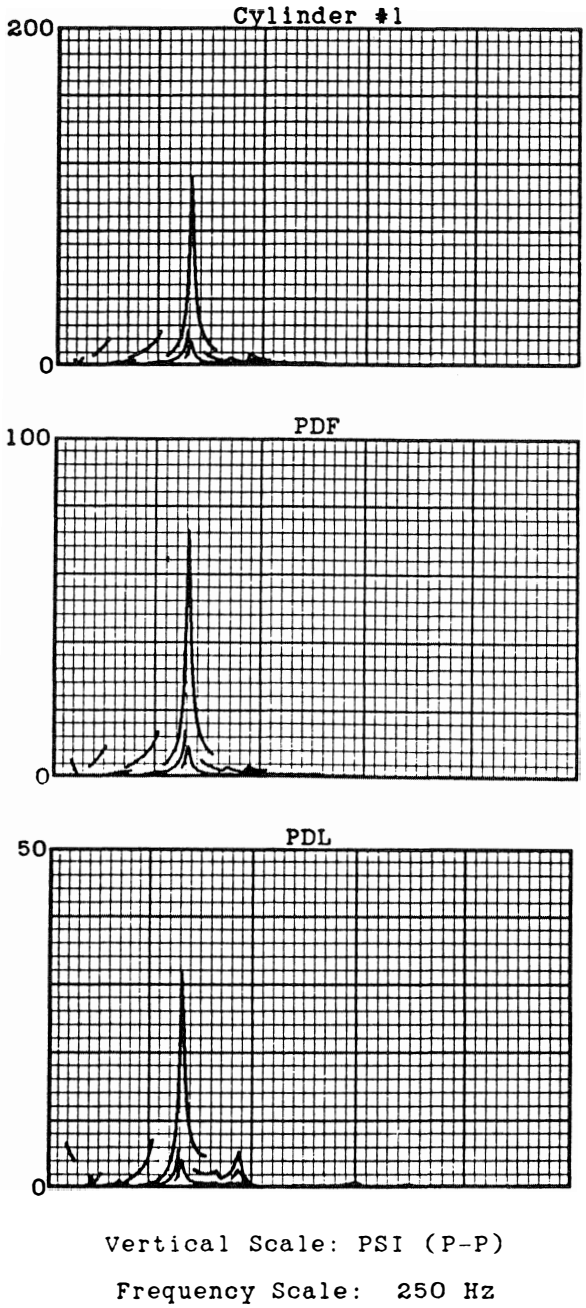

Figure 31. Predicted Pulsations in Pump and Piping System for Pump Speed Range of 170-260 CPM.

REFERENCES

1. Cook, C. P., "Shop *vs* Field Corrections to Equipment," *Proceedings of the Fourteenth Turbomachinery Symposium*, Turbomachinery Laboratories, Department of Mechanical Engineering, Texas A&M University, College Station, Texas, pp. 47-50 (October 1985).
2. Bloch, H. P., "Improving Machinery Reliability," *Practical Machinery Management for Process Plants*, Volume 1, Gulf Publishing Company, Houston, Texas, pp. 72-162 (1982).
3. McHugh, J. D., "Principles of Turbomachinery Bearings," *Proceedings of the Eighth Turbomachinery Symposium*, Gas Turbine Laboratories, Department of Mechanical En-

gineering, Texas A&M University, College Station, Texas, pp. 135-145 (November 1979).

4. Shapiro, W. and Colsher, R., "Dynamic Characteristics of Fluid-Film Bearings," *Proceedings of the Sixth Turbomachinery Symposium*, Gas Turbine Laboratories, Department of Mechanical Engineering, Texas A&M University, College Station, Texas, pp. 39-53 (December 1977).
5. Salamone, D. J., "Journal Bearing Design Types and Their Applications to Turbomachinery," *Proceedings of the Thirteenth Turbomachinery Symposium*, Turbomachinery Laboratories, Department of Mechanical Engineering, Texas A&M University, College Station, Texas, pp. 179-188 (November 1984).
6. Salisbury, R. J., Stack R., and Sassos, M. J., "Lubrication and Seal Oil Systems," *Proceedings of the Thirteenth Turbomachinery Symposium*, Turbomachinery Laboratories, Texas A&M University, College Station, Texas (November 1984).
7. Caruso, W. J., Gans, B. E., and Catlow, W. G., "Application of Recent Rotor Dynamics Developments to Mechanical Drive Turbines," *Proceedings of the Eleventh Turbomachinery Symposium*, Turbomachinery Laboratories, Department of Mechanical Engineering, Texas A&M University, College Station, Texas, pp. 1-12 (December 1982).
8. Wachel, J. C., "Rotor Response and Sensitivity," Proceedings Machinery Vibration Monitoring and Analyses, Vibration Institute, Houston, Texas, pp. 1-12 (April 1983).
9. Atkins, K. E., Tison, J. D., and Wachel, J. C., "Critical Speed Analysis of an Eight Stage Centrifugal Pump," *Proceedings of the Second International Pump Symposium, Turbomachinery Laboratories, Department of Mechanical Engineering*, Texas A&M University, College Station, Texas, pp. 59-65 (April 1985).
10. Massey, I. C., "Subsynchronous Vibration Problems in High-Speed Multistage Centrifugal Pumps," *Proceedings of the Fourteenth Turbomachinery Symposium*, Turbomachinery Laboratories, Department of Mechanical Engineering, Texas A&M University, College Station, Texas, pp. 11-16 (October 1985).
11. Childs, D. W., "Finite Length Solution for Rotordynamic Coefficients of Turbulent Annular Seals," ASLE Transactions, Journal of Lubrication Technology, *105*, pp. 437-445 (July 1983).
12. Childs, D. W. and Scharrer, J. K., "Experimental Rotordynamic Coefficient Results for Teeth-on-Rotor and Teeth-on-Stator Labyrinth Gas Seals," ASME Paper No. 86-GT-12 (1986).
13. Iwatsubo, T., Yang, B., and Ibaraki, R., "An Investigation of the Static and Dynamic Characteristics of Parallel Grooved Seals," The Fourth Workshop of Rotordynamic Instability Problems in High-Performance Machinery, Turbomachinery Laboratories, Department of Mechanical Engineering, Texas A&M University, College Station, Texas (June 1986).
14. Black, H. F. and Jenssen, D. N., "Dynamic Hybrid Properties of Annular Pressure Seals," ASME Paper 71-WA/FF-38 (1971).
15. Wachel, J. C., "Rotordynamic Instability Field Problems," Second Workshop on Rotordynamic Instability of High Performance Turbomachinery, NASA Publication 2250, Texas A&M University (May 1982).
16. Jenny, R. and Wyssman, H. R., "Lateral Vibration Reduction in High Pressure Centrifugal Compressors," *Proceedings of the Ninth Turbomachinery Symposium*, Gas Turbine Laboratories, Department of Mechanical Engineering, Texas A&M University, College Station, Texas, pp. 45-56 (December 1980).
17. Kirk, R. G. and Donald, G. H., "Design Criteria for Improved Stability of Centrifugal Compressors," Rotor Dynamic Instability, ASME Publication AME, 55 (June 1983).
18. Kirk, R. G., Nicholas, J. C., Donald, G. H., and Murphy, R. C., "Analysis and Identification of Subsynchronous Vibration for a High Pressure Parallel Flow Centrifugal Compressor," ASME Journal of Mechanical Design, Paper No. 81-DET-57 (1981).
19. Wachel, J. C. and Smith, D. R., "Experiences with Nonsynchronous Forced Vibrations in Centrifugal Compressors," Rotordynamics Instability Problems in High-Performance Turbomachinery, NASA Publication 2338, pp. 37-44 (May 1984).
20. Fulton, J. W., "Subsynchronous Vibration of Multistage Centrifugal Compressors Forced by Rotating Stall," The Fourth Workshop on Rotordynamic Instability Problems in High-Performance Turbomachinery, Turbomachinery Laboratories, Department of Mechanical Engineering, Texas A&M University, College Station, Texas (June 1986).
21. Barrett, L. E., Gunter, E. J., and Nicholas, J. C., "The Influence of Tilting Pad Bearing Characteristics on the Stability of High Speed Rotor-Bearing Systems," *Topics in Fluid Film Bearing and Rotor Bearing Systems, Design and Optimization*, ASME Publication Book No. 100118, pp. 55-78 (1978).
22. Wachel, J. C., et al., "Rotordynamics of Machinery," Engineering Dynamics, Incorporated, Report EDI 86-334 (April 1986).
23. Stroh, C. G., "Rotordynamic Stability-Simplified Approach," *Proceedings of the Fourteenth Turbomachinery Symposium*, Turbomachinery Laboratories, Department of Mechanical Engineering, Texas A&M University, College Station, Texas, pp. 3-10 (October 1985).
24. Frej, A., Grgic, A., Heil, W., and Luzi, A., "Design of Pump Shaft Trains Having Variable-Speed Electric Motors," *Proceedings of the Third International Pump Symposium*, Turbomachinery Laboratories, Department of Mechanical Engineering, Texas A&M University, College Station, Texas, pp. 33-44 (May 1986).
25. Wachel, J. C., et al., "Vibrations in Reciprocating Machinery and Piping," Engineering Dynamimcs, Incorporated, Report EDI 85-305 (October 1985).
26. Szenasi, F. R., and Von Nimitz, W., "Transient Analysis of Synchronous Motor Trains," *Proceedings of the Seventh Turbomachinery Symposium*, Gas Turbine Laboratories, Department of Mechanical Engineering, Texas A&M University, College Station, Texas, pp. 111-117 (December 1978).
27. Wachel, J. C., Von Nimitz, W., and Szenasi, F. R., "Case Histories of Specialized Turbomachinery Problems," *Proceedings of the Second Turbomachinery Symposium*, Gas Turbine Laboratories, Department of Mechanical Engineering, Texas A&M University, College Station, Texas, pp. 35-50 (October 1973).
28. VanLaningham, F. L. and Wood, D. E., "Fatigue Failures of Compressor Impellers and Resonance Excitation Testing," *Proceedings of the Eighth Turbomachinery Sympo-*

sium, Gas Turbine Laboratories, Department of Mechanical Engineering, Texas A&M University, College Station, Texas, pp. 1-9 (November 1979).

29. Bultzo, C., "Analysis of Three Impeller Failures: Experimental Techniques used to Establish Causes," *Proceedings of the Fourth Turbomachinery Symposium*, Gas Turbine Laboratories, Department of Mechanical Engineering, Texas A&M University, College Station, Texas, pp. 31-38 (October 1975).
30. Sohre, J. S., "Steam Turbine Blade Failure, Causes and Corrections," *Proceedings of the Fourth Turbomachinery Symposium*, Gas Turbine Laboratories, Department of Mechanical Engineering, Texas A&M University, College Station, Texas, pp. 9-30 (October 1976).
31. Sparks, C. R. and Wachel, J. C., "Pulsations in Liquid Pump and Piping Systems," *Proceedings of the Fifth Turbomachinery Symposium*, Gas Turbine Laboratories, Department of Mechanical Engineering, Texas A&M University, College Station, Texas, pp. 55-61 (October 1976).
32. Smith, D. R., and Simmons, H. R., "Unique Fan Vibration Problems: Their Causes and Solutions," *Proceedings of the Ninth Turbomachinery Symposium*, Gas Turbine Laboratories, Department of Mechanical Engineering, Texas A&M University, College Station, Texas, pp. 33-43 (December 1980).